Applied Energy 113 (2014) 324–333

Contents lists available at ScienceDirect

Applied Energy

journal homepage: www.elsevier.com/locate/apenergy

Parametric study and simulation of a heat-driven adsorber for air conditioning system employing activated carbon–methanol working pair

Harunal Rejan Ramji [a], Sing Lim Leo [b], Mohammad Omar Abdullah [a,*]

[a] Department of Chemical Engineering and Energy Sustainability, Faculty of Engineering, Universiti Malaysia Sarawak (UNIMAS), 94300 Kota Samarahan, Sarawak, Malaysia
[b] International College of Advanced Technology Sarawak (ICATS), Jalan Canna, Off Jalan Wan Alwi, Tabuan Jaya, 93350 Kuching, Sarawak, Malaysia

HIGHLIGHTS

- Wall thickness affecting adsorbent bed temperature thus adsorption capacity.
- Higher input temperature required longer cycle time but produce higher cooling power.
- Wall thickness of 15–20 mm offer suitable heat transfer rate and desorption temperature.
- A cooling power of 0.65 kW and COP around 0.25 associated with cycle time of 1200 s.

GRAPHICAL ABSTRACT

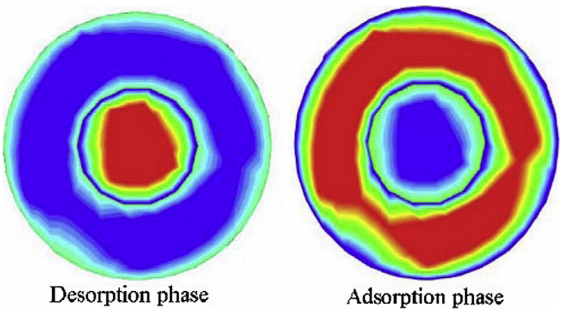

ARTICLE INFO

Article history:
Received 19 April 2013
Received in revised form 27 June 2013
Accepted 6 July 2013
Available online 15 August 2013

Keywords:
Activated carbon
Adsorption air conditioning system
CFD
Cooling power
COP

ABSTRACT

Objectives: This paper aims to present a parametric study to compare with the experimental results obtained previously for a typical activated carbon–methanol, adsorption air-conditioning system powered by exhaust heat. The main objective is to study the effect of wall thickness on the desorption temperature and the cooling performance.
Methods: The current study is a simulation/parametric investigation employing computational fluid dynamics (CFD) simulation technique.
Results: It is found that the CFD result is close to the experimental works. In this CFD investigation, an input exhaust gas of 200 °C would have bed temperature around 120 °C while employing 20 mm thick of wall made by stainless steel. The adsorber took around 10 min to heat up and decrease to room temperature around the same period. This set of data produce a cooling power of 0.65 kW and COP around 0.25 with cycle time of 1200 s.
Conclusion: It is concluded that higher input temperature would have relatively longer cycle time but it is able to produce higher cooling power in return. While in design, it proves that an optimal wall thickness should be 15–20 mm of stainless steel that offer lower heat transfer rate to maintain the system under functional T_{des} at all time.
Practice implications: This paper proves that adsorption air-conditioning system is technically applicable; however wall thickness of the adsorber should be considered seriously as one of the important parameters for suitable heat transfer and improved adsorption–desorption rate of the system.

* Corresponding author. Tel.: +60 82 583280; fax: +60 82 583409.
E-mail addresses: amomar13@gmail.com, amomar@feng.unimas.my (M.O. Abdullah).

0306-2619
http://dx.doi.org/10.1016/j.apenergy.2013.07.017

Nomenclature

A	cross sectional area (m^2)
A_{lm}	log mean area
C_p	specific heat capacity ($J\,kg^{-1}K^{-1}$)
COP	coefficient of performance
h	convective coefficient
k	constant in Dubinin equation
m	mass (kg)
P	cooling power (kW)
Q	cooling capacity (kJ)
q_v	vaporization heat
SCP	specific cooling power
T	temperature (°C)
t	time (s)
x	concentration ($kg\,kg^{-1}$)
x_o	initial concentration ($kg\,kg^{-1}$)

Subscript

ac	activated carbon
ads	adsorption
*cyc*1/2	half cycle
eg	exhaust gas
exp	experimental
des	desorption phase
ev	evaporator
i	inside
o	outside
ref	refrigerant (methanol)
s	saturated
v	vaporization

Superscript

n	constant in Dubinin equation

1. Introduction

The progress in the automobile air-conditioning systems which utilize the adsorption cooling technology had progressed ever since early 90s. The conventional electrical-driven compression systems are widely use in almost all of the automobiles today. However, air-conditioning technology is required to evolve due to the new environmental regulations, notably Montreal Protocol in 1987, Kyoto Protocol in 1997 and European Commission Regulation 2037/2000. These regulations are concerning about the depletion of the ozone layer and also global warming, which decided to phase- out CFCs and followed by HCFCs and HFC-134a. As a result, this trend has led to a strong demand for a new air-conditioning technology Leo and Abdullah [1]. Unfortunately, no working prototype has been practically run in present automobiles due to various restrictions, due to sizing and cooling capacity limitations Abdullah et al. [2].

A review on solar refrigeration by Kim [3] had covered the subjects of discussion on the energy efficiency and economic feasibility of solar base cooling technologies. It is stated that solar sorption systems appeared to be cheaper than electric and thermo-mechanical system. This is then evidently proven in literature involving adsorption refrigeration cycle powered by solar energy or other waste heat exhausted from engines. Solar adsorption refrigeration had been quite successfully used for ice making and cold production.

Wang and Oliveira [4] designed and tested an icemaker which is able to produce ice between 4 and 7 kg per meter square of solar collector. The generated COP is recorded at 0.2–0.6 region. Apart from that, there are also research on solar absorption chillers for space cooling, e.g. by Ritcher and Safarik [5]. The presented COP by the author is recorded at 0.27 with a cooling power of 15 kW. Other literatures provides solar adsorption ice maker by Boubakri et al. [6], silica gel–water adsorption refrigeration cycle driven by waste heat of near-ambient temperature Saha et al. [7], zeolite–water solar cold storage system Lu et al. [8], and a combined solar thermoelectric- adsorption cooling system using activated carbon–methanol working pair Abdullah et al. [9]. Based on the cited literatures, extensive research has been performed on adsorption refrigeration, but research on the possibility of applying this technology for automobile air-conditioning purposes is still rare.

In a research performed by Suzuki [10] associated with the application of adsorption cooling systems to automobiles have clarify the feasibility of this system. Though the relevant data was presented and it shows compelling results but the author only performed simulations study only; unfortunately, no experimental work was carried out to verify his claim. In another case, an experimental analysis of the applicability of an adsorption system for electric vehicle air conditioning was carried out by Aceves [11]. In his findings the coefficient of performance (COP) of the system employing zeolite and water as a working pair was approximately 0.28. His studies indicated that conventional compression air conditioners were superior to adsorption systems due to their higher COPs and are more compact in size. The drawback of using zeolite and water as a working pair is that a very low operating pressure is needed.

Meanwhile, Sato et al. [12] have presented a multiple-stage adsorption air-conditioning system for vehicles. Although the efficiency of the multiple-stage adsorption system was improved, the size of the system also increased and its control system became more complex. Zhang [13] has described an experimental intermittent adsorption cooling system driven by the waste heat of a diesel engine. Zeolite 13×-water was used as the working pair and a finned double-tube heat exchanger was used as the adsorber. The COP and specific cooling power (SCP) of the system is 0.38 and 25.7 W/kg, respectively. Wang et al. [14] have studied an adsorption air conditioning for a bus driven by waste heat from exhausted gases. The working pair for this system is activated carbon and ammonia with the cooling power of 2.58 kW and a COP of 0.16. The activated carbon is pressurized to a density of about 900 kg/m^3 into fit additional adsorbent into the adsorber. The total weight of the two adsorbers is about 248 kg and occupied about 1.0 m^2.

In another research conducted by Lu et al. [15], they had presented their experimental studies on the practical performance of an adsorption air-conditioning system powered by exhausted heat from a diesel locomotive. The system was incorporated with one adsorbent bed and utilizes zeolite and water as a working pair to provide chilled water for conditioning the air in the driver's cab of the locomotive. Their experimental results showed that the adsorption system is technically feasible and can be applied for space air conditioning. Under typical running conditions, the average refrigeration power ranging from 3.0 to 4.2 kW has been

Table 1
D–A equation constant values for appointed working pair [14].

Working Pair	k	x_0	n
Zeolite–Water	5.36	0.26	1.73
Activated carbon–ammonia	3.57	0.29	1.38
Activated carbon–methanol	13.38	0.45	1.5

obtained. However, this system may not be suitable for automobile application due to its size and high regenerative temperature.

According to Leo and Abdullah [1] in their research findings on automobile adsorption application, the coefficient of performance (COP) obtained thru experimentation is approximately 0.19. Theoretically the value is quite small in compare to regular air conditioning that is on the market now. In spite of this, the value of specific cooling power recorded was a promising 396.6 W kg^{-1}. Other considered data acquired along were the cycle time which is set at 20 min and average chilled air produced is around 22.6 °C. The prototype operates intermittently between two adsorbers in order to retain the chilled air along the 20 °C temperature line. Being able to produce this degree of air conditioning, the cooling coil temperatures can fell up to 9.5–14.7 °C.

This paper is a continuation of study by Leo and Abdullah [1] and Abdullah et al. [2] on adsorption cooling system. In previous papers, the authors had discussed the basic prototype design and conducted several relevant experimental works and successfully patented a working prototype. In this paper, however, simulation works by CFD are presented and discussed ways to achieve more favorable design and minimize unnecessary energy losses. In attaining the specified condition, parametric study based on three temperature inlet is implemented. By varying these temperatures, the corresponding variables such as adsorption rate, heat transfers and operating cycle time can be obtained. Subsequently, optimization study is conducted to verify the findings.

2. Physical and mathematical model

2.1. The adsorber

The Dubinin–Astakhov (D–A) equation relates the concentration, and temperature can be represented in the form of Lu et al. [15].

$$x = x_0 \exp\left(-k\left(\frac{T}{T_s}-1\right)^n\right) \tag{1}$$

where x, represents the concentration of methanol adsorbed in bed at the T temperature of the adsorption. T_s represents the saturated temperature in the adsorber with given P, pressure. The saturated adsorption capacity of the working pair is given by x_o. The parameter k and n are constant that varies with different working pair. Table 1 provides the values of the parameters constant according to its working pair given by Deshpande and Pillai [16].

2.2. Mass and energy balance equation

2.2.1. Adsorption rate

The adsorption process in this system can be divided into two phase which are desorption (regeneration) phase and also the adsorption phase itself. In this system, these two identically design adsorber will be operating intermittently with each other. The cycle time will rely heavily on the adsorption and desorption rate of the system as given below Tso et al. [17].

Adsorption:

$$\frac{dx_{ads}}{dt} = K_{ads}(x_{ads,eq} - x_{ads}) \tag{2}$$

$$x_{ads} = x_{ads,eq} - (x_{ads,eq} - x_{ads,o})\exp(-K_{ads}t) \tag{3}$$

Table 2
Antoine equation constant values for the given refrigerant[16].

Compounds	Temperature range	A	B	C
Methanol	(−20–140)	7.87863	1473.11	230

Desorption:

$$\frac{dx_{des}}{dt} = K_{des}(x_{des}) \tag{4}$$

$$x_{des} = x_{des,eq} - (x_{des,eq} - x_{des,o})\exp(-K_{des}t) \tag{5}$$

2.2.2. Condenser and evaporator model

In modeling the condenser and evaporator, several assumptions were considered given as followings,

1. The working fluid is considered always in thermodynamic equilibrium corresponding to its saturation conditions.
2. The saturated temperature depends on the internal pressure of the working equipments given by Antoine equation with parameter as given in Table 2 given by Felder and Rousseau [18].
3. Assumable that the entire refrigerant fluid flow rate coming from the condenser is instantly evaporated. There will be no fluid lost in between the process. Every amount of refrigerant desorbed in the first adsorber will be transferred in completion to the next adsorber where adsorption took place.

This means;

$$m_{ref} = x_{des}m_{ac} \tag{6}$$

While employing the usual energy equation, the total heat power input to the system including the condenser and evaporator models can be presented as below:

Total heat power input

$$P = \dot{m}_{eg}C_{p,eg}(T_{eg,in} - T_{eg,out}) \tag{7}$$

Condenser

$$\dot{m}_{ref}c_{p,ref}(T_{des} - T_{cond}) + h_{v,ref} = \dot{m}_{air}c_{p,air}(T_{out} - T_{in}) \tag{8}$$

Evaporator

$$h_{v,ref} - \dot{m}_{ref}c_{p,ref}(T_{cond} - T_{ev}) = \dot{m}_{air}c_{p,air}(T_{in} - T_{out}) \tag{9}$$

2.3. System performance parameters

2.3.1. Cooling power and cooling capacity

The cooling output readings of the prototype via experiment are calculated from measuring the temperature difference of the inlet and outlet of the chilled air by its flow rate and specific heat Lu et al. [15].

$$P_{\exp} = \dot{m}_{chill}c_{p,air}(T_{chill,in} - T_{chill,out}) \tag{10}$$

The total cooling capacity will be

$$Q_{c,\exp} = \int P_{\exp}dt \tag{11}$$

While in simulation, cooling power can be obtained theoretically by equations given:

$$Q_{c,theo} = m_{ref}(q_{v,ref} - c_{p,ref}(T_{cond} - T_{ev})) \tag{12}$$

Hence, the total cooling capacity can be presented as;

$$p_{theo} = \frac{m_{ref}}{t_{cyc1/2}}(q_{v,ref} - c_{p,ref}(T_{cond} - T_{ev})) \tag{13}$$

where $q_{v,ref}$ is the heat of evaporation for methanol, and $t_{cyc1/2}$ is the half cycle time of the whole operation.

2.3.2. Coefficient of performance (COP) and specific cooling power (SCP)

The performance of the adsorption cooling system is commonly evaluated using two performance factors; the coefficient of

performance (COP) and specific cooling power (SCP). In general, COP is the amount of cooling produced by an adsorption cooling system per unit heat supplied by Lu et al. [15] as shown:

$$\mathrm{COP} = \frac{Q_{ev}}{Q_{in}} \tag{14}$$

The SCP, on the other hand, is defined as the ratio between the cooling production and the cycle time per unit of adsorbent weight, as given below Leo and Abdullah [1]:

$$\mathrm{SCP} = \frac{Q_{ev}}{(m_{ac})} \tag{15}$$

Since SCP relates to both the mass of adsorbent and the cooling power, it reflects the size of the system. For a nominal cooling load, higher SCP values indicate the compactness of the system.

2.4. Governing equations

In simulation, fluid flow modeling described by Siegal and Howel [19] had been utilize to solve the classic Navier–Stokes equations by superimposing thousands of grid cells which described the physical geometry of the air flow and heat transfer, i.e.;

$$\frac{d}{dt}(\rho\varphi) + \nabla(\rho v\varphi - \psi^{\varphi}\nabla\varphi) = S\varphi \tag{16}$$

The transport equations for mass conservation, momentum and energy for any system can be given in these generic equations Abdullah et al. [20]:

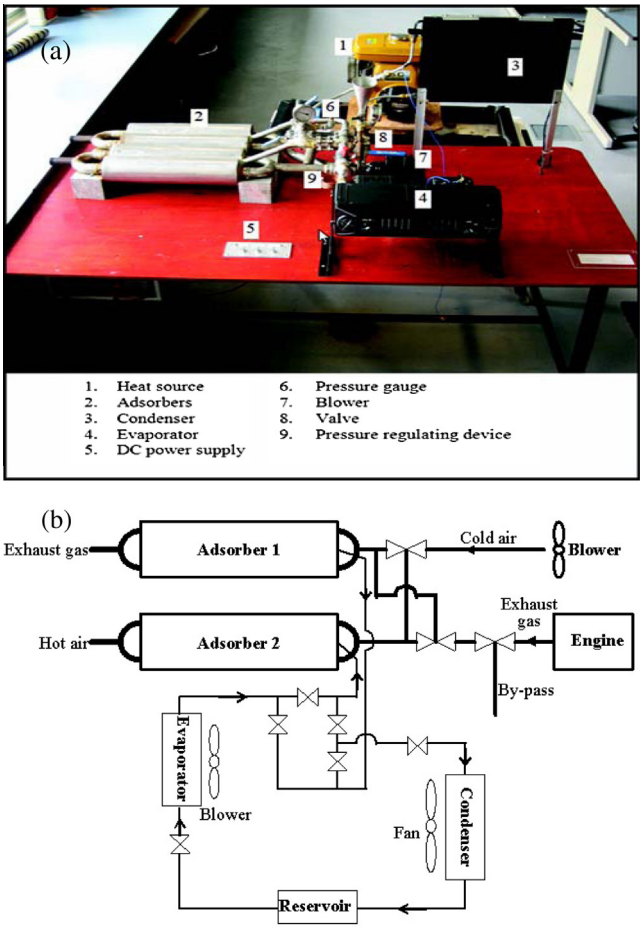

Fig. 1. (a) Experimental prototype rig [1]; (b) schematic diagram of the prototype.

Continuity:

$$\frac{d\rho}{dt} + \frac{d(\rho u_i)}{dx_i} = 0 \tag{17}$$

Momentum:

$$\frac{d(\rho v_i)}{dt} + \frac{d(\rho v_i v_j)}{dx_i} = -\frac{dP}{dt} + \frac{d\tau_{ij}}{dx_i} \tag{18}$$

Energy:

$$\frac{d}{dt}(\rho c_P T) + \frac{d}{dx_i}(\rho c_P T) = \frac{d}{dx_i}\left(k\frac{dT}{dx_i}\right) + \frac{dp}{dt} + \frac{dp}{dx_i} \tag{19}$$

The simultaneous equations thus form are solved iteratively for each one of the cells to produce a solutions which satisfied the conservation law of mass, momentum and energy.

3. Design and experimental work

In the previous study done by Leo and Abdullah [1], the prototype constructed was composed of regular air-conditioning equipments, particularly vehicle cooling system. The most crucial and complex part in the prototype is the adsorbers. In this study, the ANSYS 13.0 Design Modeller, pre processor software was used to design the adsorbers.

The adsorbers were designed in such a way (see Figs. 1 and 2) to maximize the quantity of activated carbon and to improve the heat transfer between the adsorbent and exhaust gas. Two identical adsorbers were constructed, each adsorber consisting of two adsorbent beds. Each adsorbent bed was packed with approximately 0.8 kg of granular palm-activated carbon in a stainless steel net. The dimensions of the adsorbers are 40 cm in length, 20 cm in width, and 10 cm in height is visualized in Fig. 3. Six radial stainless steel fins symmetrically distributed in the adsorbent bed are employed to intensify heat conduction. While for evaporator simulations, a simple heat exchanger model template are used to evaluate the results. Every relevant result obtained from the adsorber simulations would be further progresses to the evaporator model.

The prototype utilized a four-stroke petrol 5HP (3.7 kW) engine to supply the heat source required during the regeneration process. The heat from the exhaust gas can reach over 150.0 °C, which was more than enough to operate the prototype. The condenser used is a type of air-finned-tube aluminum heat exchangers that is attached with a 12 V d.c. fan to increase the heat rejection rate. Meanwhile, a hanging type of air-finned-tube aluminum heat exchanger, which consists of a cooling coil of 3412 Btu/h (1.0 kW) and two blowers powered by a 12 V d.c. motor with a motor speed controller were integrated to the prototype. The detail design of the complete system is given in Abdullah and Leo [21].

Fig. 1 shows the placement and integration of the components in the prototype, which consists of two adsorbers, a blower, an evaporator attached to two blowers, a condenser attached to a fan, an expansion valve, four check valves, three three-way valves, an engine, and several pipe connectors. Before the prototype is ready to be tested, it is evacuated and charged with 455 mL of methanol. The quantity of methanol charged was lower compared to the adsorption capacity of activated carbon in order to prevent the activated carbon from becoming saturated, which could reduce the system performance.

This prototype generally works in two main phases, i.e. desorption phase and adsorption phase. Practically the cooling effect was due to the adsorption process; while desorption on the other hand worked as pre-cooling in the operation as to prepare the adsorbent for the adsorption process. Throughout this processes, desorption and adsorption have to work continuously in a suitable time limit which often referred to as time cycle. Hence, to achieve this condi-

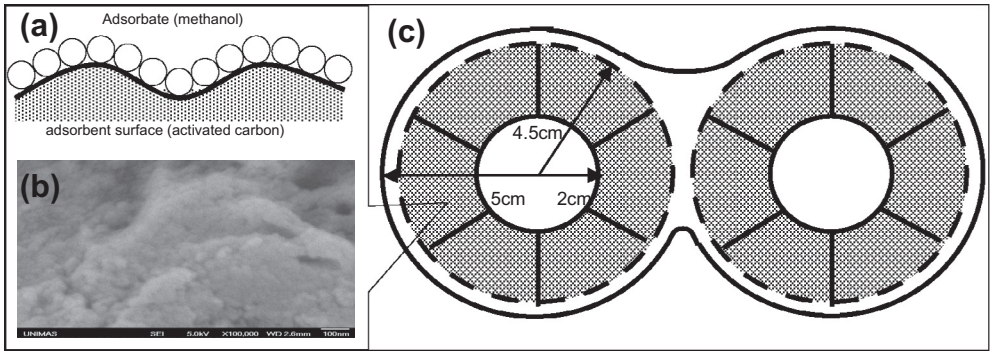

Fig. 2. The adsorber. (a) graphical illustration of adsorbent and adsorbate inside the adsorber; (b) SEM image of palm-derived activated carbon; (c) adsorber cross section diagram showing the dimension used.

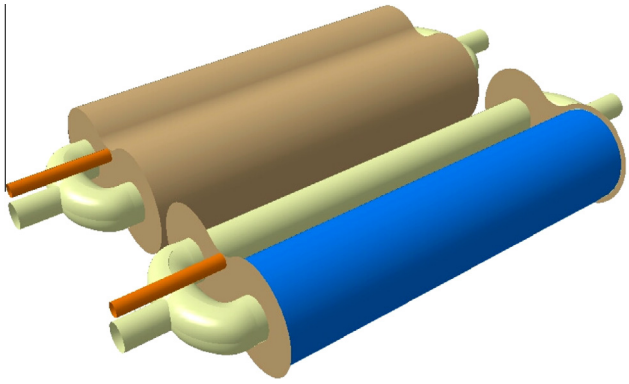

Fig. 3. Design of the adsorber using CATIA 3D [1].

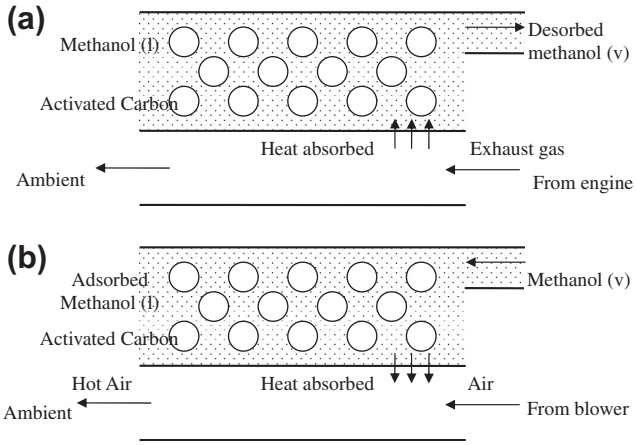

Fig. 4. Simplified (a) desorption and; (b) adsorption mechanism that occurs inside the adsorber. The circles represent the activated carbon granular. The shaded region indicates the liquid methanol.

tion an intermittent operation was designed whereby two adsorbers of same design were used. The idea is that whenever one of the adsorber undergoing adsorption, the second adsorber would undergo desorption. Thru this scheme, a continuous cooling can be provided by this system.

4. Simulation results and analysis

During the heating process, methanol is desorbed and pressurized from the adsorber. Initially, the adsorber is injected with 455 mL of methanol which is equivalent to 360 g in standard atmospheric pressure condition. Theoretically, the more methanol are desorbed the more cooling effect can be produced. Equivalently, the ability of methanol to be squeezed out of the adsorbent bed will indicate the effectiveness of the system's heat transfer processes.

In Fig. 4a, the diagram illustrates the early condition of the adsorber when the activated carbon and methanol in room temperature around 30 °C. Once exhaust gas has entered the area, the heat of the exhaust gas would vaporize the methanol within the activated carbon. Thus the pressurized methanol would be released from the adsorber due to pressure difference making its way to evaporator. In this condition the adsorber was in desorption process. While in Fig. 4b, the adsorption process took place at the same time but on the second adsorber desorption takes place. The diagram shows that the source of heat now is from the methanol and activated carbon side. This heat is transferred to the cool air blown by the blower to hasten the cool down process. This is essential to reduce the cycle time of the operation.

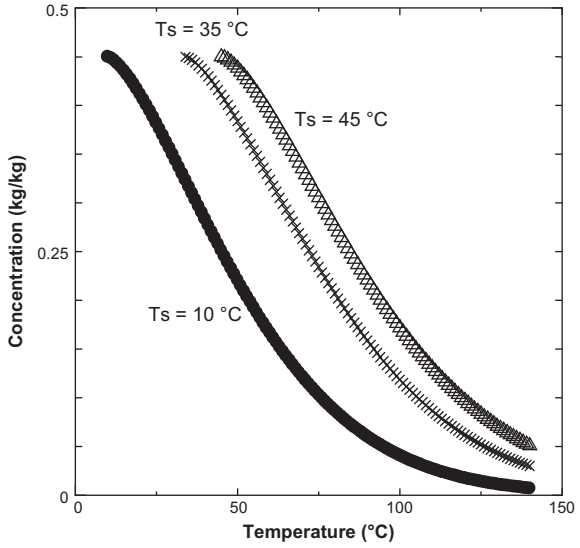

Fig. 5. Adsorption capacity isobar of activated carbon–methanol.

The ratio between adsorbate and adsorbent in this system was set around 0.45:1, which means the methanol content inside the adsorber was around 45% of the adsorbent content. It is to be noted

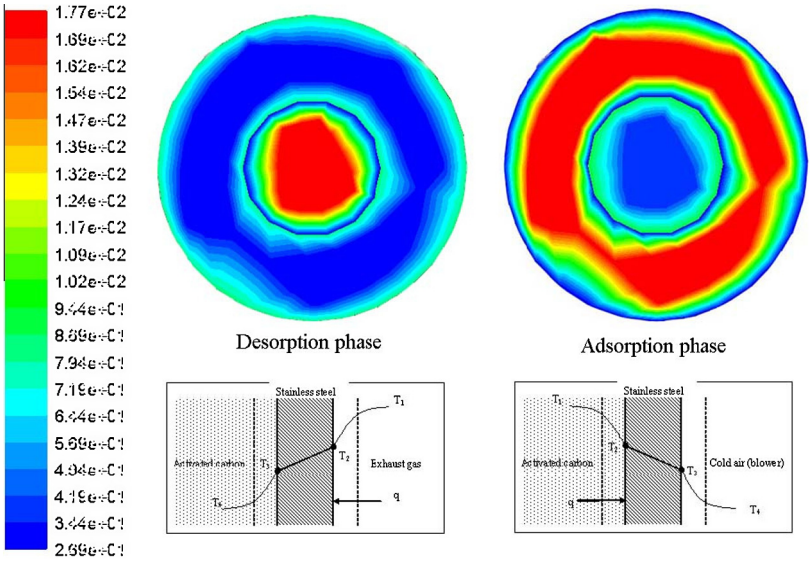

Fig. 6. Temperature profile of adsorber cross section during desorption and adsorption.

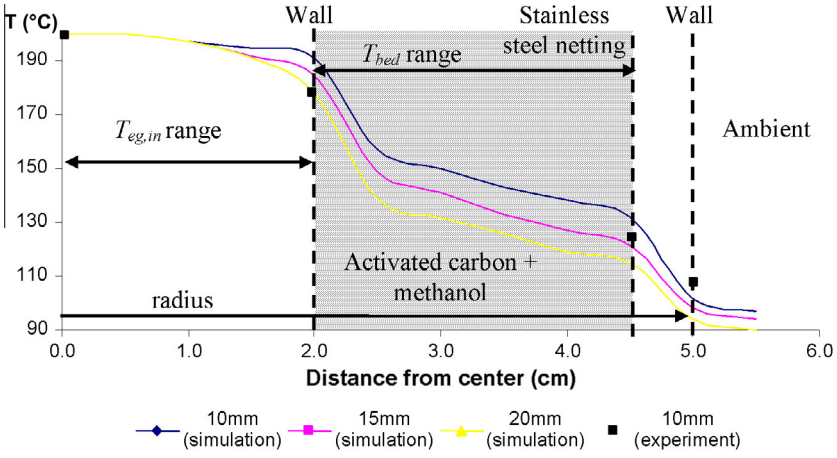

Fig. 7. Internal temperature of the adsorber during the desorption phase.

that an excess amount of adsorbate can cause over saturation of activated carbon that could lead to reduce of system performance Leo and Abdullah [1].

4.1. Adsorption isobar

In Fig. 5 the adsorption isobars for the working pair of activated carbon–methanol are presented. The saturated temperature, T_s used were in corresponds to the saturated pressure, P_s that were probable to the system. Implementing the D–A equation, the simulated equilibrium adsorption capacity of activated carbon–methanol can be expressed as:

$$x_{eq} = 0.45 \exp\left(-13.38\left(\frac{T}{T_s} - 1\right)^{1.5}\right) \quad (20)$$

The usage of activated carbon–methanol as the adsorption pair is not advisable for operation above the temperature of 150 °C, as methanol would decompose due to catalytic reaction at this temperature [15]. So in order to apply this working pair in this prototype, the operating temperature of the system has to be maintained below the decomposition temperature to avoid the loss of the refrigerant in the system.

Table 3
Parameters values adopted in the adsorber simulation.

Parameters	Value	Unit
Moving exhaust gas heat transfer coefficient, h_i	33.15	W/m^2 K
Stainless steel 316 L thermal coefficient, k	16.3	W/m K
Activated carbon + methanol, h_o	1.515	W/m^2 K
Exhaust gas mass flow rate, m	0.014	kg/s
Exhaust gas heat capacity, C_p	1.063	kJ/kg K

4.2. Desorption phase

Desorption temperatures, T_{des} for the system depends on the bed temperature of the adsorber, T_{bed}. While, the rate of desorption rely on the adsorber bed pressure, P_{bed} which is assume in saturated condition in first place during the operation and will be constant thru out the process. The findings were plotted based on the concentration of methanol in the adsorber during desorption phase, x_{des} and the average internal temperature of the adsorber, T_{bed} in a period of time. The shifting of desorption and adsorption process rely on the ability of the adsorber to desorbed methanol out which is also called regeneration phase. When methanol desorption come to completion, the system will switch to adsorption and cooling air was used to cool the heated adsorber.

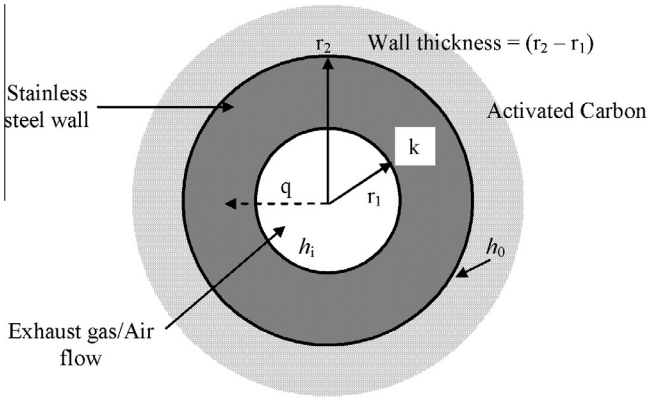

Fig. 8. Simple cut through diagram of the adsorber.

Table 4
Settable operating condition.

T_{in} (°C)	T_{des} (°C)	T_{ads} (°C)
150	<90	40
200	<120	40
250	<150	40

4.2.1. Effect of wall thickness on Adsorber bed temperature, T_{bed}

Figs. 6 and 7 depict the adsorber bed temperature T_{bed} of the adsorber. This case study was presented via CFD simulation in comparison with the prototype experimental result conducted in laboratory. It would be difficult to obtain internal temperature profiles of the adsorber experimentally, so the experimental data (at 10 mm wall thickness) was taken only at external wall of the adsorber. Hence by using simulation the temperature contour is shown vividly to compliment that was obtained experimentally (Fig. 7). Fig. 8 is a schematic diagram showing the heat transfer mechanism inside the adsorber.

The CFD result in Fig. 7 has shown that 10 mm of wall thickness would provide higher undesired heat channeling. Thus to maintain T_{bed} is in optimum operational range of T_{des} (below 150 °C) for the working pair, a wall of greater thickness should be chosen to keep T_{bed} as low as possible to avoid methanol decomposition. $T_{eg,in}$ utilized in this simulation model were 150, 200 and 250 °C.

For the simulation works, the bed temperature T_{bed} is obtained through the equation described by Geankoplis [22].

$$q = \frac{T_{in} - T_{bed}}{\sum R} \tag{21}$$

$$T_{bed} = T_{in} - q\sum R \tag{22}$$

$$q = mC_p\Delta T \tag{23}$$

$$\sum R = \left[\left(\frac{1}{h_i A_i}\right) + \left(\frac{r_o - r_i}{kA_{lm}}\right) + \left(\frac{1}{h_o A_o}\right)\right] \tag{24}$$

The parameters involved in this equation were expressed in Table 3 with its given values.

4.2.2. Temperature of the heat source, $T_{eg,in}$, the adsorber bed temperature, T_{bed} and adsorbate concentration, x_{des}

The graphs in Fig. 9 were plotted to show the relationships of concentration of the adsorber, x_{des} and adsorber bed temperature, T_{bed}, as a function of cycle time and at three different input exhaust gas temperatures (i.e. $T_{eg,in}$ at 150, 200 and 250 °C). The run time was set for 25 min. So the times taken for desorption and adsorption processes can be identified between these three set of trials. Table 4 shows the operating conditions of the system.

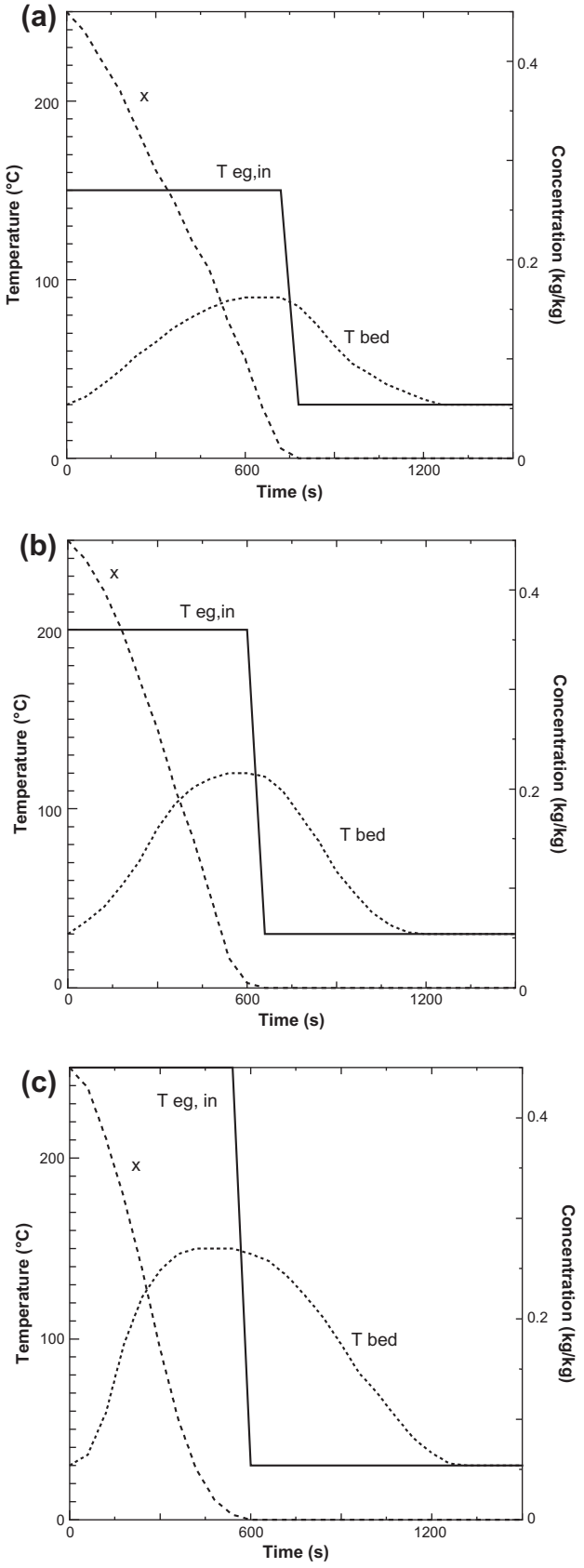

Fig. 9. Concentration of adsorbate (methanol), x inside the adsorber and bed temperature, T_{bed} in isobaric condition, (a) 150 °C, (b) 200 °C, (c) 250 °C.

Table 5
Evaporator parameters.

$T_{chill,in}$	30 °C
m_{air}	0.045 kg/s
$C_{p,air}$	1.005 kJ/kg °C

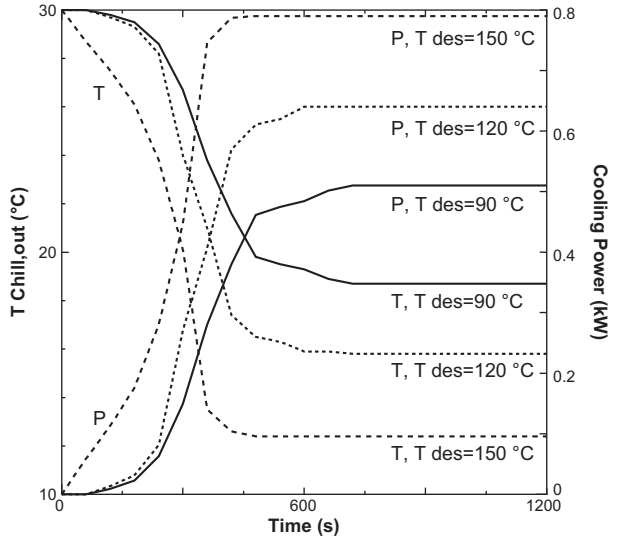

Fig. 10. Comparison of different T_{des} effect to $T_{chill,out}$ and its cooling power.

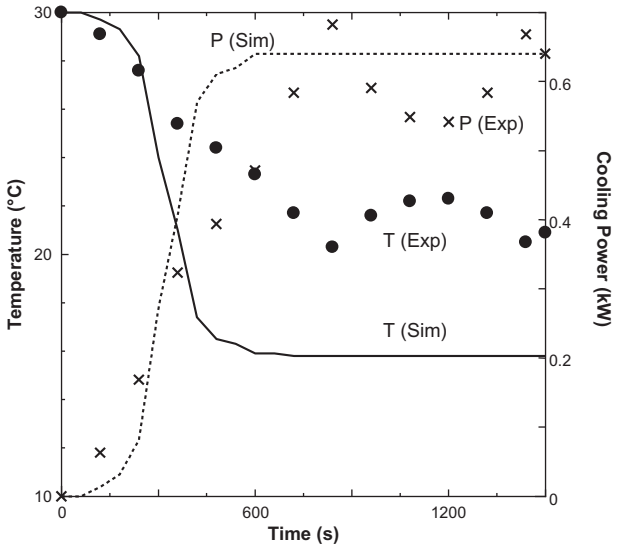

Fig. 11. Comparison between experimental and simulation results on $T_{chill,out}$ and their respective cooling power, P.

In an isobaric condition, when the input temperature $T_{eg,in}$ was 150 °C (Fig. 9a), concentration, x of the methanol in the adsorber took longer time to decrease. At a higher input temperature $T_{eg,in}$ is 250 °C (Fig. 9c), methanol can be desorbed at a faster rate. The desorption rates is several minutes faster at 200 °C (Fig. 9b) then 150 °C (Fig. 9a). It can be interpreted that higher $T_{eg,in}$ would increase of the adsorber bed temperature T_{bed}. Hence, x_{des} against time will be much shorter, hence the cycle time, as a result of which flow rate of methanol m_{ref} is increased. The explanation for this condition is that when heating is done at higher temperature, vaporization rate would take place at a much faster rate. This is in accordance to the rule of energy equilibrium, where energy is transferred between bodies/compounds i.e. activated carbon – exhaust gas to achieve balance/stability of the system. In this case, exhaust gas which possess relatively higher temperature level transmitted this higher thermal energy to the lower temperature level of the methanol liquid.

4.3. Chill temperature release, $T_{chill,out}$ and cooling power, P_{theo}

The chill temperature, $T_{chill,out}$ simulated profiles as a function of time is as shown in Fig. 10. The graph depicts that when T_{des} is low, chilled temperature produce would be higher hence lower cooling power. While utilizing higher T_{des} would produce higher cooling power and lower $T_{chill,out}$. The parameters of evaporator used in the modeling are given in Table 5. While in Fig. 11, simulation and experimental results were compared to observe its coherency. It was found that simulation results and the experimental results shows a slightly different values of $T_{chill,out}$. This may be due to the effect of ambient temperature that could affect the measuring of $T_{chill,out}$. This error could provide a slightly different reading from the simulation results. Though cooling power for both results exhibits satisfactory coherency.

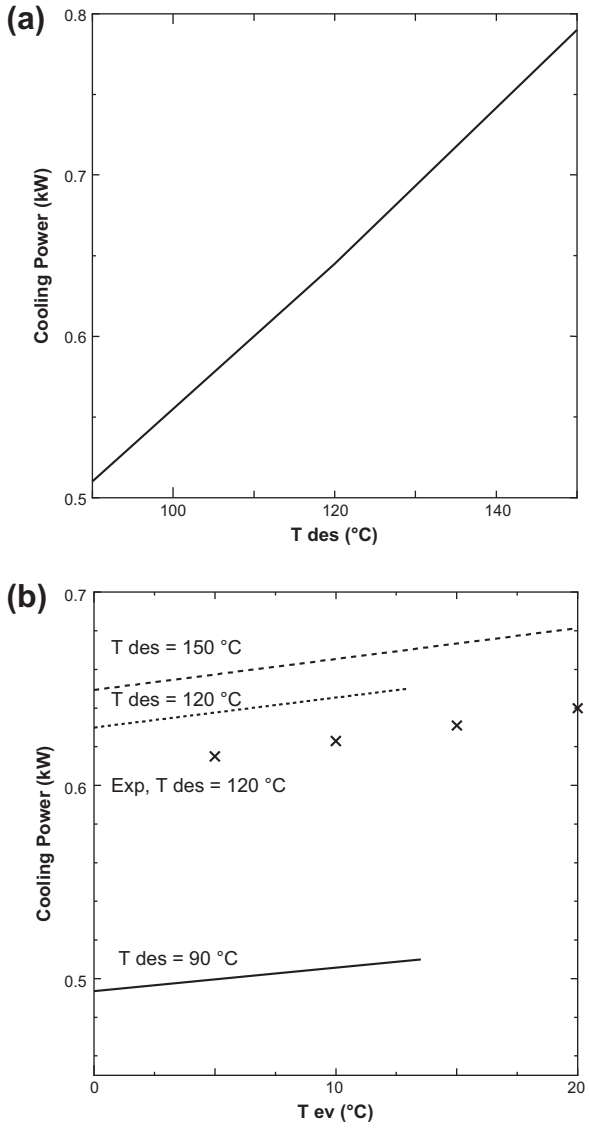

Fig. 12. (a) Influence of desorption temperature, T_{des} on cooling power (b) Influence of evaporating temperature, T_{ev} on cooling power.

Table 6
Comparison of experimental set up an simulation for the prototype adsorbers.

	Experimental Set Up [1]	Simulation design (Present study)			Lu et al. [15]
Mass of adsorbent (g)	800 (in each adsorber) of activated carbon				140,000 of 13× zeolite grain
Mass of adsorbate (g)	360 of methanol				185,000 of water
Length (cm)	40				100
Width (cm)	20				150
Height (cm)	10				45
Exhaust gas temperature (°C)	<200	150	200	250	400–600
Desorption temperature (°C)	120	<90	<120	<150	270
Adsorption temperature (°C)	40	40	40	40	34,40
Desorption cycle time (s)	600	720	600	540	3600
Adsorption cycle time (s)	600	600	600	600	7200
Total cycle time (s)	1200	1320	1200	1140	10800
Cooling Power (kW)	0.635	0.52	0.64	0.79	3.0–4.2
COP	0.19	0.27	0.25	0.25	0.18–0.21
SCP (W/kg)	396.6	324.78	400.00	493.75	25.71

4.4. Influence of desorption temperature, T_{des} and evaporating temperature, T_{ev}

Fig. 12a shows the simulation cooling power at different desorption temperature. According to the figures, the cooling power is greater at higher T_{des}. However, it is to be noted that the practical maximum temperature should be maintained below the decomposition temperature of the pair i.e. below 150 °C.

Fig. 12b shows the effect of evaporator temperature on the system cooling power. The graph indicates that when the evaporator temperature T_{ev} increased the cooling power of the system would slightly increase as well. The experimentation works were carried out at 120 °C while the simulated cooling power values were done at desorption temperatures of 90, 120, and 150 °C, respectively. Now at 120 °C, the experimental cooling power obtained slightly lower than the simulation cooling power at same desorption temperature. This is probably due to the impact of pressure changes in the actual experiment where saturated temperature changes with pressure change thus the adsorption capacity of activated carbon–methanol working pair. Similar phenomenon had been described by Cho and Kin [23].

5. Discussions

As we put together the findings on these two adsorbers, one of the most significance aspects to be considered is the cycle time of the operation. While previously during the development of the prototype, all of the operations were done manually and on a try and error basis. But through CFD investigation using ANSYS 13.0 software, these aspects can be thoroughly take notice and its effect to the whole system. The parameters were provided in Table 6. The values of the given parameters were obtained through simulations previously discussed above.

Desorption temperature is essential in calculating the SCP and COP of this adsorption cooling system which all depends heavily on m_{ref}. To have a good cooling, desorption temperature must be in an optimum range hence a higher COP. System cooling performances can be increased by implementing continuous heat recovery cycle that is by having the use of two intermittently operating adsorber. The heat recovered by these dual bed adsorbers could further improve the COP of the system [24]. Apart from that, much quicker cycle is necessary for high values of SCP. The most desirable conditions for optimum adsorber design are as follows Abdullah et al. [2].

1. Light and conveniently small (low adsorbent and adsorbate contain).
2. Wall thickness preferably 20–30 mm of stainless steel.
3. Short cycle time.

Guided by these parameters as given in Table 6, an optimal design of a practical adsorber with the shortest total cycle time can thus be obtained. Stated at the first consideration was the mass of the adsorber which include the activated carbon and methanol content. Though the overall system ideally has to be light and small (minimize the amount of activated and methanol), the amount of adsorbent and adsorbate, however, must also be adequate to provide sufficient cooling. Deficient amount of this pair would lead to insufficient cooling and the desired cooling could not be achieved. In the above study, the optimization suggested by the simulation can be listed into;

1. Higher $T_{eg,in}$ would yield higher cooling power, P but T_{bed} must be below operational T_{des} of the working pair to avoid the decomposition of the refrigerant.
2. The optimum T_{ev} falls under 15–25 °C region to produce maximum cooling.
3. Higher T_{des} have faster desorption rate and this cut the cycle time shorter.

Based on Table 6, a comparison was made between three distinct researches that include the experimental prototype by Leo and Abdullah [1], diesel locomotive waste-heat powered adsorption Lu et al. [15] and simulation study via CFD based on Leo and Abdullah [1]. In Lu's findings, the author had presented a functional adsorption air conditioning system powered by waste heat. All of the results produced show a lot promise and its feasibility to be introduced as a regular cooling system. Though, the design as extravagantly huge and heavy which could than affect the performance of the car. Therefore, Leo and Abdullah [1] decided to use a reduced sizing and weight system by introducing a dual adsorber system which can work intermittently with each other. The solution leads to a smaller system.

Depend on compactness and sizing, a practical automobile adsorption system would perhaps need to acquire a COP range from 0.25 to 0.8, with SCP from 0.4–1 kW/kg. Suggested cycle time for a dual adsorber system shall be <10–15 min to avoid overheating of adsorber and loss of refrigerant.

7. Conclusions

Based on the CFD result, it shows that the prototype application in real world would be feasible and a stepping edge in environmentally friendly technology. Through the CFD analysis conducted, an

input exhaust gas of 200 °C would have bed temperature around 120 °C while employing 30 mm thick of wall made by stainless steel. The adsorber took around 10 min to heat up and decrease to room temperature around the same period. This set of data produce a cooling power of 0.65 kW and COP around 0.25 with cycle time of 1200s. It is summarized that higher input temperature would have relatively longer cycle time but it is able to produce higher cooling power in return. While in design, it proves that an optimal wall thickness should be 20–30 mm of stainless steel that offer lower heat transfer rate to maintain the system under operational T_{des} at all time.

Acknowledgements

This present study was supported by the Ministry of Higher Education, Malaysia under Prototype Development Research Grant Scheme (PRGS), Contract No: PRGS/1/11/TK/UNIMAS/02/01. The authors would like to thank all staff for their continuous encouragements throughout this project.

References

[1] Leo SL, Abdullah MO. Experimental study of an automobile exhaust heat-driven adsorption air-conditioning laboratory prototype by using palm activated carbon–methanol. HVAC&R Res 2010;16(2):221–31.
[2] Abdullah MO, Tan IAW, Leo SL. Automobile adsorption air-conditioning system using oil palm biomass-based activated carbon: a review. Renew Sust Energy Rev 2011;15:2061–72.
[3] Kim DS, Infante Ferreira CA. Solar refrigeration options – a state of the art. Int J Refrig 2008;31(1):3–15.
[4] Wang RZ, Oliveira RG. Adsorption refrigeration – an efficient way to make good use of waste heat and solar energy. Prog Energy Combust Sci 2006;32:424–58.
[5] Richter L, Safarik M. Solar cooling with ammonia water absorption chillers. In: Proceedings of international conference solar air conditioning; Bad Staffelstien, Germany.
[6] Boubakri A, Guilleminot JJ, Meunier F. Adsorptive solar powered ice maker: experiments and model. Sol Energy 2000;69(3):249–63.
[7] Saha BB, Akisawa A, Kashigawi T. Solar/waste heat driven two-stage adsorption chiller: the prototype. Renew Energy 2001;23(1):93–101.
[8] Lu YZ, Wang RZ, Zhang M, Jiangzhou S. Adsorption cold storage system with zeolite-water working pair used for locomotive air conditioning. Energy Convers Manage 2003;44(10):1733–43.
[9] Abdullah MO, Ngui JL, Hamid KA, Leo SL, Tie SH. Cooling performance of a combined solar thermoelectric-adsorption cooling system: an experimental study. Energy Fuels 2003;23:5677–83.
[10] Suzuki M. Application of adsorption cooling systems to automobiles. Heat Recov Syst CHP 1993;13(4):335–40.
[11] Aceves SM. Analytical comparison of adsorption and vapor compression air conditioners for electrical vehicle applications. Energy Resources Tech Trans ASME 1996;118(1):16–20.
[12] Sato H, Honda S, Tanaka H, Terao T. Adsorptive type refrigeration apparatus. US patent 5619866; 1997.
[13] Zhang LZ. Design and testing of a waste heat adsorption cooling system. Appl Therm Eng 2000;20(1):103–14.
[14] Wang RZ, Wang W, Qu TF. Research and development on waste heat driven adsorption bus air conditioning system. Final Report SJTU-UTRC Joint Research Program, Shanghai Jiao Tong University (SJTU) and United Technologies Research Center (UTRC). China; 2001.
[15] Lu YZ, Wang RZ, Jianzhou S, Xu YX, Wu JY. Practical experiments on an adsorption air-conditioner powered by exhausted heat from a diesel locomotive. Appl Therm Eng 2004;24:1051–9.
[16] Deshpande AC, Pillai RM. Adsorption air conditioning (AdAC) for automobiles using waste heat recovered from exhaust gases. In: 2nd Int Conference on Emerging Trends in Eng. and Tech. ICETET-09 IEEE; 2009. p. 19–24.
[17] Tso CY, Chao CYH, Fu SC. Performance analysis of a waste heat driven activated carbon composite adsorbent–water adsorption chiller using simulation model. Int J Heat Mass Transfer 2012;55:7596–610.
[18] Felder RM, Rousseau RW. Elementary principles of chemical processes, 3rd ed., John Wiley & Sons, Inc.; 2000. p 640–1.
[19] Siegal R, Howel JR. Thermal Radiation Heat Transfer. 3rd ed. New York: Hemisphere; 1992 [Chapter 7].
[20] Abdullah MO, Mikie FA, Lam CY. Drying performance and thermal transient study with solar radiation supplemented by force-ventilation. Int J Therm Sci 2006;45:1027–34.
[21] Abdullah MO, Leo SL. Heat driven adsorption air-conditioning system for automobile. Malaysian Patent Number: PI20081641; MY-143033-A; 2009.
[22] Geankoplis CJ. Principles of steady-state heat transfer. Transport Processes and Separation Process Principles fourth ed. Prentice Hall PTR; 2003. p. 235–46 [Chapter 4].
[23] Cho SH, Kin JN. Modeling of a silica gel/water adsorption cooling system. Energy 1992;17:829–39.
[24] Wang RZ. Performance improvement of adsorption cooling by heat and mass recovery operation. Int J Refrig 2001;24:602–11.